

Providence, RI
NOISE-CON 2016
2016 June 13–15

Measured Noise from Small Unmanned Aerial Vehicles

Randolph Cabell*, Robert McSwain† Ferdinand Grosveld‡
NASA Langley Research Center Northrop Grumman Corp.
Hampton, VA 23681 Hampton, Va 23681

ABSTRACT

Proposed uses of small unmanned aerial vehicles (UAVs), including home package delivery, have the potential to expose large portions of communities to a new noise source. This paper discusses results of flyover noise measurements of four small UAVs, including an internal combustion-powered model airplane and three battery-powered multicopters. Basic noise characteristics of these vehicles are discussed, including spectral properties and sound level metrics such as sound pressure level, effective perceived noise level, and sound exposure level. The size and aerodynamic characteristics of the multicopters in particular make their flight path susceptible to atmospheric disturbances such as wind gusts. These gusts, coupled with a flight control system that varies rotor speed to maintain vehicle stability, create an unsteady acoustic signature. The spectral variations resulting from this unsteadiness are explored, in both hover and flyover conditions for the multicopters. The time varying noise, which differs from the relatively steady noise generated by large transport aircraft, may complicate the prediction of human annoyance using conventional sound level metrics.

1. INTRODUCTION

Small unmanned aerial vehicles (UAVs) have many potential benefits to society including infrastructure inspection, farming, security, and small package shipping. As the possible uses of these small vehicles are beginning to be explored, the potential community impact, both visually and aurally, from repeated close-proximity flights of these vehicles is also beginning to be explored.

As part of an effort to better understand the noise characteristics of small UAVs, NASA conducted outdoor flight tests to measure the noise from a few representative UAVs. These measurements will be used in future research to understand limitations of and development needs for noise prediction tools applied to this scale of vehicles, and guide planning for future psychoacoustic tests to understand possible unique aspects of annoyance due to noise from these vehicles. Basic acoustic measurements were made on four small commercially available UAVs, including a fixed-wing airplane, a tricopter, a quadcopter, and a hexcopter, where the numerical prefix indicates the number of rotors on each vehicle. Noise characteristics such as spectral content, sound levels at fixed distances, and the time varying nature of the sound field are discussed. Some challenges encountered making acoustical measurements from these vehicles are discussed, including the difficulty of obtaining accurate vehicle position information.

*randolph.h.cabell@nasa.gov

†robert.g.mcswain@nasa.gov

‡f.grosveld@nasa.gov



Figure 1: Tested vehicles(l to r: Y6, Edge 540, Phantom 2, Hex Flyer)

Vehicle Name	Type	Flight Weight (kg)	Max Speed (m/s)	Power	Location
Edge 540 ¹	fixed-wing	~11.3	27	gas engine	42VA
DJI Phantom 2 ²	quadcopter	1.6	15	electric motor	42VA
3DR Y6 ³	tricopter	2.5	15	electric motor	42VA
Prioria Hex ⁴	hexcopter	7.3	15	electric motor	AP Hill

Table 1: Tested Vehicles

The paper begins with a description of the two flight tests and four vehicles flown during those tests, followed by discussion of basic spectral characteristics of the four vehicles. Time varying spectral characteristics for hover and flyovers are discussed next for the quadcopter and hexcopter, including some electric motor noise. Noise metrics, including L_{Amax}, EPNL, and SEL are discussed for some of the vehicles, and the importance of accurately determining the vehicle altitude is discussed.

2. VEHICLE AND FLIGHT TEST DESCRIPTION

Acoustic measurements on small UAVs were made in two separate flight tests at two different locations. The first test, conducted in December 2014, took place at the Virginia Beach Airport (42VA), a privately-owned airfield with a 1477 m-long, 58 m-wide grass runway. The second test, conducted in August 2015, took place at Finnegan Airfield at Fort AP Hill, Virginia. Finnegan Airfield is dedicated to small UAVs and has a 365 m-long, 30 m-wide paved runway.

The four vehicles discussed here are shown in Figure 1; specifics of the vehicles are listed in Table 1. The commercial names of the vehicles are listed in the first column. The flight weight for each vehicle includes the weight of a 590 g flight data acquisition system (FDAS) that was used to record vehicle state and position information. The flight weight for the hexcopter also includes a 1.4 kg loudspeaker used for a separate acoustic test. Note that the FDAS weight is nearly twice the maximum payload weight recommended by the manufacturer of the quadcopter (DJI). Although this did not present any issues with handling qualities, it is reasonable to assume that the noise signature with this payload will be different from the same vehicle without the payload. These differences would include lower blade passage frequencies due to less thrust being required to keep the vehicle in the air. The effects of unsteady blade loading may also be more pronounced on the tested quadcopter than on a more lightly loaded one.

Flight trajectories included level flyovers by all vehicles at various altitudes and speeds and

hovers of the multicopters at various altitudes. Not all of these flights yielded high quality acoustic data, particularly flights flown at 42VA, due to noise from a military airport 8 km away and other noise sources unrelated to the flight test. All vehicles were flown manually during the acoustic measurements, so a human pilot, not an autopilot, was in control of each vehicle at all times. The pilot may have caused additional unsteadiness in the vehicle flight path relative to an auto-piloted vehicle as the human pilot adjusted the vehicle position to maintain station or achieve a target flyover altitude.

The tested vehicles all have fixed-pitch propellers. The airplane has a single propeller for propulsion while the multicopters have from three to six propellers for lift and thrust. Attitude of the airplane is controlled using conventional control surfaces including ailerons, elevators, and a rudder. Attitude of the multicopters (roll, pitch, and yaw) is controlled by varying the rotation speed of the fixed pitch propellers to produce thrust variations about a desired axis. The specific rotor speed variations are determined by the flight control system on each vehicle in response to pilot commands or to maintain attitude in response to an external disturbance such as a wind gust.

A. Flight Data Acquisition System

Vehicle state information including position and attitude (roll, pitch, yaw) was recorded with a detachable 3DR Pixhawk flight data acquisition system (FDAS).⁵ The vehicle position, recorded with standard GPS accuracy of 4 m rms,⁶ was recorded at a 5 Hz rate. To more precisely locate these small vehicles during post-flight data processing, a Swift Navigation Piksi GPS unit featuring real-time kinematics (RTK) functionality was also mounted on each vehicle.⁷ The Piksi system, henceforth referred to as the RTK system, consists of a base unit mounted at a known point on the ground and a rover unit attached to the vehicle. The system relies on carrier phase tracking and is capable of centimeter relative positioning of the base and rover units under ideal conditions. The base and rover units each have GPS antennas and a radio frequency link between them for more reliable carrier phase tracking. The relative position of the base and rover is recorded at a rate of 10 Hz.

Operational experience with the RTK system revealed that good localization performance required careful system initialization and required that the base and rover units observe the same satellites in the GPS constellation. Momentary shielding of the GPS antenna such that part of the sky was obscured on either the base or the rover would usually prevent a good position solution. Such shielding can be a problem when a vehicle experiences large roll or pitch excursions that momentarily obscure the GPS antenna. Each RTK position observation includes a status bit indicating quality of the RTK solution.

Data acquired by the FDAS and Piksi systems were time-stamped with GPS time. Leap seconds were subtracted from these GPS times to obtain UTC time for synchronization with the acoustic data.

B. Acoustic Instrumentation

Acoustic instrumentation for the two tests consisted of 1/2" pre-polarized, random-incidence microphones on acrylic ground boards. The ground boards were 41 cm in diameter with a thickness of 1.9 cm. Each microphone was covered with a hemispherical foam windscreen. An array of either three or four microphones was placed in a line transverse to the runway center-line (three ground microphones were used at 42VA; four microphones were used at AP Hill). Microphone locations

were surveyed for the AP Hill test and thus their locations were assumed to be accurate to within a centimeter. At 42VA the microphone locations were measured with standard GPS equipment and placed relative to airfield markers at known locations, so their locations were known to an accuracy of about 50 cm. For hovers and flyovers, the pilot was instructed to center the vehicle's flight path over one of the microphones.

The microphone responses were digitized using a portable USB data acquisition system with a sampling rate of 20 kHz connected to a laptop computer. An external GPS receiver with a time code generator provided a UTC time signal acquired simultaneously with the acoustic data for post-flight synchronization with FDAS data.

All measured microphone data reported here were halved to account for assumed pressure doubling by the ground board.

3. RESULTS

Results are discussed for measurements made with the microphone closest to the vehicle during hover and flyover maneuvers. For hovers this microphone was approximately under the vehicle, whereas for flyovers the pilot was told to center the vehicle's flight path over this microphone. The vehicle position for the cases discussed here was determined using the RTK positioning system. The RTK and GPS position data agreed to within 2 meters horizontally and 5 meters vertically when the RTK status bit indicated a good RTK solution. When the status bit did not indicate a good solution, the RTK position varied significantly from the GPS solution; none of these cases are discussed here. The FDAS on the Y6 tricopter malfunctioned during all but a few hover flights so discussion of data from that vehicle is limited.

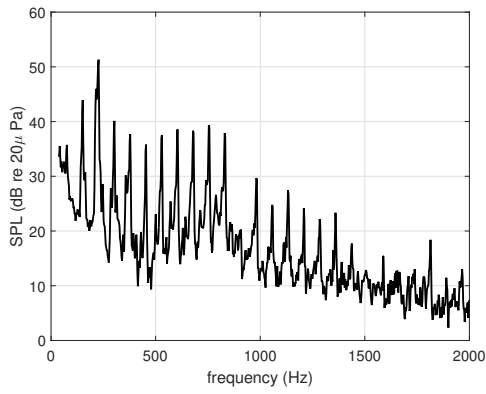
A. Basic Spectral Characteristics

Figure 2 shows basic spectral characteristics of the sound pressure level (SPL) of each vehicle up to 2 kHz. Each spectrum was computed from seven seconds of time data using Hanning-windowed, 8192-point segments with 50% overlap between neighboring segments, for a bin width of 2.4 Hz.

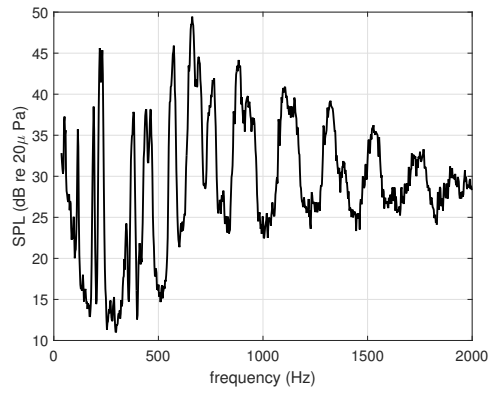
The measured noise of all four vehicles is dominated by propeller-related noise, including narrowband deterministic noise and broadband noise. Deterministic, or periodic, noise sources include thickness noise, loading noise, and unsteady force noise.^{8,9} These noise sources produce tones at harmonics of the blade passage frequency (BPF) corresponding to the narrowband peaks in the spectra. The multicopter spectra all have significant noise at higher harmonics of the BPF, and in some cases the levels at higher harmonics exceeds levels at the BPF. Unsteady force noise that occurs on a periodic basis, for example from disturbed inflow due to other rotors or the fuselage, is an important source of noise at higher harmonics of the blade passage frequency^{8,9} and may explain the high levels at these higher harmonics. Broadband noise is also an important noise source for these vehicles, including noise caused by unsteady pressure fluctuations due to turbulence and boundary layer interactions with the edges of the blade.⁹

The nominal blade tip Mach number for each vehicle, M_{tip} , listed in the figure captions, was less than 0.3 for the multicopters and was about 0.5 for the airplane. For comparison, full-scale helicopter blades have advancing-side tip Mach numbers from 0.6 to 0.7,⁸ and airplane propellers generally have even higher tip Mach numbers.

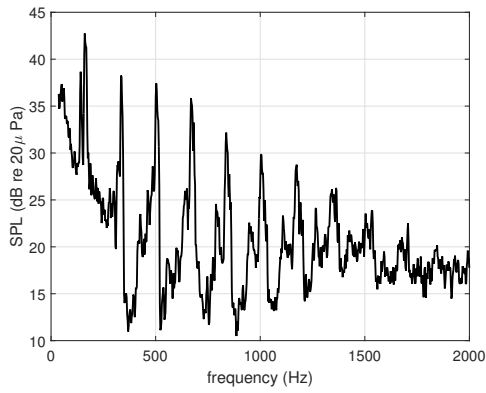
The peaks at BPF harmonics in the fixed-wing spectrum, Figure 2a, are generally narrower than in the multicopter spectra. The increased broadness of the tones in the multicopter spectra is



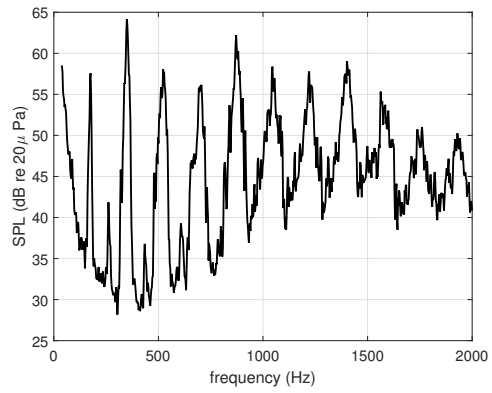
(a) Fixed-wing approach ($M_{tip} \sim 0.5$).



(b) Quadcopter hover ($M_{tip} \sim 0.2$).



(c) Tricopter hover ($M_{tip} \sim 0.2$).



(d) Hexcopter hover ($M_{tip} \sim 0.3$).

Figure 2: Example spectra of tested vehicles.

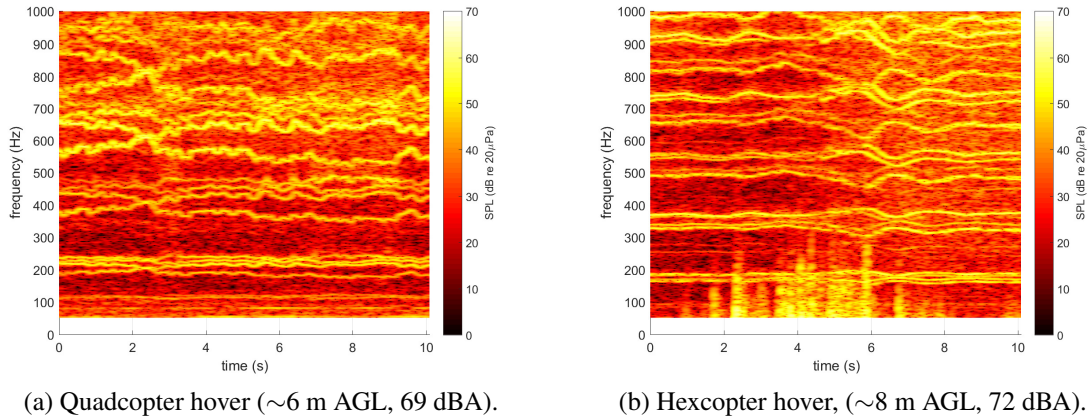


Figure 3: Spectrograms of multicopter hovers.

due to at least two factors: the presence of multiple rotors operating at closely spaced frequencies will spread energy in the spectrum. In addition, rotor speed variations due to the flight control system that occur within the spectral analysis window will also spread energy in the spectrum. These speed variations are used by the flight control system to adjust the vehicle’s attitude, hence they occur nearly continuously in an outdoor environment where wind is present.

B. Time-Varying Spectral Characteristics: Hover

Spectrograms showing frequency behavior with time are revealing for these small vehicles where unsteady behavior is common. Figure 3 shows 10-second spectrograms for hovers of the quadcopter and hexcopter (the average altitude above ground level (AGL) and A-weighted SPL over the 10 second segment are shown in the figure caption). The spectrograms are rich with harmonics of the BPF, near 200 Hz for both vehicles. Four distinct spectral lines can be seen in Fig 3a near 200 Hz, one for each rotor on the quadcopter. The rotor rotational speeds are not exactly equal due to minor variations in blade and motor properties, offsets to the vehicle center of gravity, and wind. Small variations with time in the BPFs are magnified at higher harmonics, hence at several hundred Hertz the spectrum is a mix of various harmonics of rotor BPFs.

The spectrogram for the hexcopter, in Figure 3b, is similar to the quadcopter but the BPFs, located just below 200 Hz, are nearly equal so it is difficult to see a distinct line for each rotor. The BPFs appear to be more steady with time for the hexcopter than for the quadcopter, which could be due to the hexcopter’s greater inertia, less sensitivity to wind, or even lower winds during the hexcopter test. The increase in low frequency broadband noise in the spectrogram from about 2 seconds to 6 seconds was caused by downwash from the vehicle as it drifted around the measurement microphone.

C. Time-Varying Spectral Characteristics: Flyover

Noise data was also collected for flyovers of the fixed-wing vehicle and the multicopters. In nearly all of the flyovers post-test analysis revealed a tendency of the pilots to fly an altitude profile that started and ended above the microphone flyover point, instead of flying a more desirable constant altitude trajectory. Although the pilots were instructed to maintain a constant altitude during the

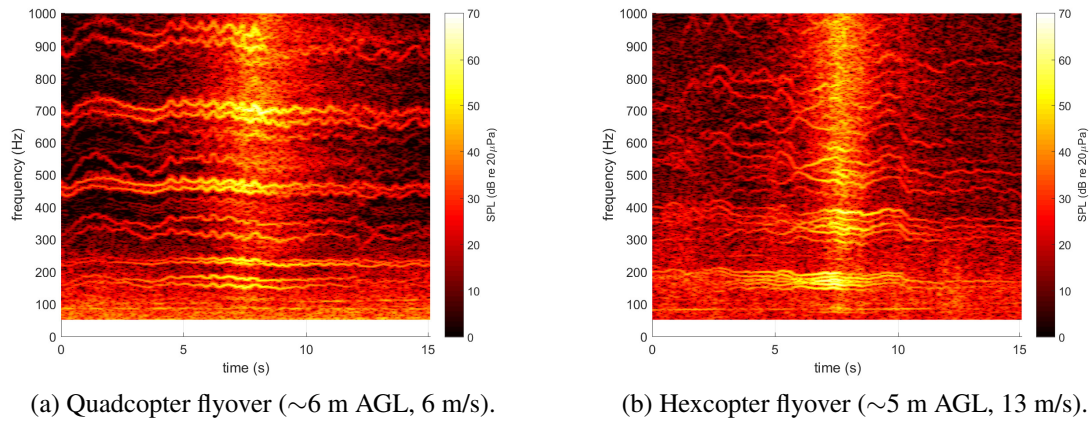


Figure 4: Spectrograms of multicopter flyovers.

flyover, this was very difficult to do using only visual cues when the vehicle was more than a few tens of meters away from the pilot. Altitude callbacks from an observer watching flight telemetry were used on early flights, but the callbacks were easily audible on the measurement microphones and were stopped. An autopilot may be the best solution to this issue.

Spectrograms for flyovers of the quadcopter and hexcopter are shown in Figure 4. Tones are still prominent in the spectrograms, and the broadband noise level is well below the tones except at the point of closest approach, which occurred at about 7 seconds in both plots. A more subtle difference between the hover and flyover spectrograms is the separation of BPFs that occurs in order to maintain forward flight. Specifically, in order for the quadcopter to maintain forward flight, the rear rotors are driven at a higher rotational speed to produce more lift than the front rotors. The difference in rotor speeds appears in the spectrogram as two BPFs below 200 Hz and two just above 200 Hz. This difference in rotor speeds was especially pronounced on the tested vehicle due to the FDAS payload being mounted below the vehicle, creating an offset between the aerodynamic center and the center of gravity of the vehicle. This offset required greater thrust from the rear propellers to pitch the vehicle forward and produce forward motion. In addition, note that the sound pressure levels of rear rotor harmonics, at 450 Hz, 675 Hz, and 900 Hz, appear to be higher than BPF harmonics of the front rotor at 350 Hz and 525 Hz. The BPF harmonics are prominent even at the point of closest approach when broadband noise is highest.

Variations in the BPFs of the hexcopter rotors are not as large as on the quadcopter, but six distinct BPFs are apparent in parts of Figure 4b near 200 Hz. The harmonics of the hexcopter seem to fade into the background noise more quickly than those of the quadcopter, including at the point of closest approach when broadband noise increases.

The time-history of the A-weighted SPL during the flyovers, computed at 0.5-second intervals, is shown in Figure 5. Although the quadcopter is much lighter than the hexcopter, its sound levels are consistently higher than the hexcopter. The A-weighted spectrum for each vehicle at the time segment corresponding to the maximum A-weighted level is shown in Figure 6. The broadband noise of the hexcopter is higher than that of quadcopter, but the quadcopter spectrum has prominent BPF harmonics between 500 and 1000 Hz that result in a higher A-weighted SPL.

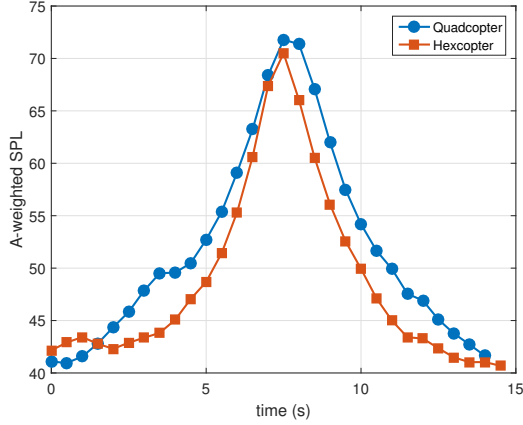


Figure 5: A-weighted SPL at 0.5-second intervals during flyover.

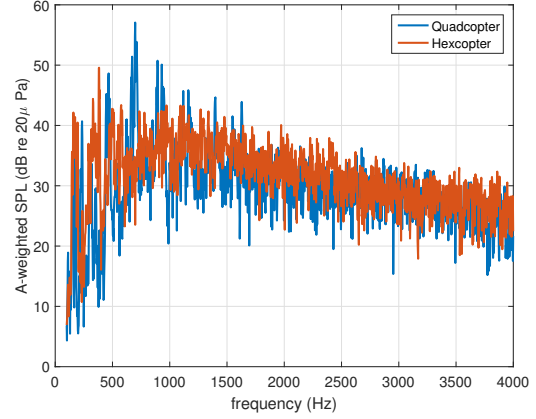
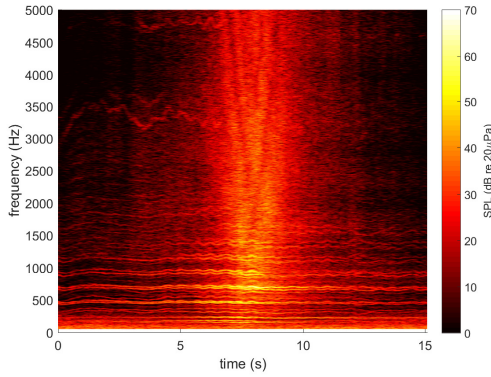
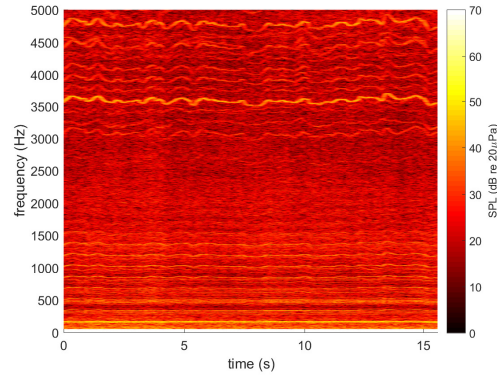


Figure 6: A-weighted spectra at L_{Amax} in Figure 5.



(a) Quadcopter flyover (~6 m AGL, 6 m/s).



(b) Tricopter hover (~6 m AGL).

Figure 7: High frequency spectrograms of multicopter flights.

D. High Frequency Electric Motor Noise

High frequency noise presumably caused by the electric motors was audible during many of the multicopter flights. These vehicles are driven by brushless DC motors, with a metallic housing containing permanent magnets rotating around a fixed armature. Noise from these motors can be caused by force pulses as the magnets and armature interact, and variations in forces caused by phase changes in the motor drive signal.¹⁰ Spectrograms showing the SPL up to 5 kHz of the quadcopter and tricopter are shown in Figure 7. High frequency tones are visible in both figures near 3500 Hz and below 5000 Hz. Although atmospheric absorption at these high frequencies will attenuate such noise, it could still be an important part of the annoyance experience when the vehicle operates close to humans.

E. Noise Metrics

Two metrics commonly applied to conventional passenger transport aircraft are the maximum A-weighted sound pressure level (L_{Amax}), and the Effective Perceived Noise Level (EPNL), a noise metric with tone and duration corrections.¹¹ Values of L_{Amax}, adjusted to a flyover altitude of

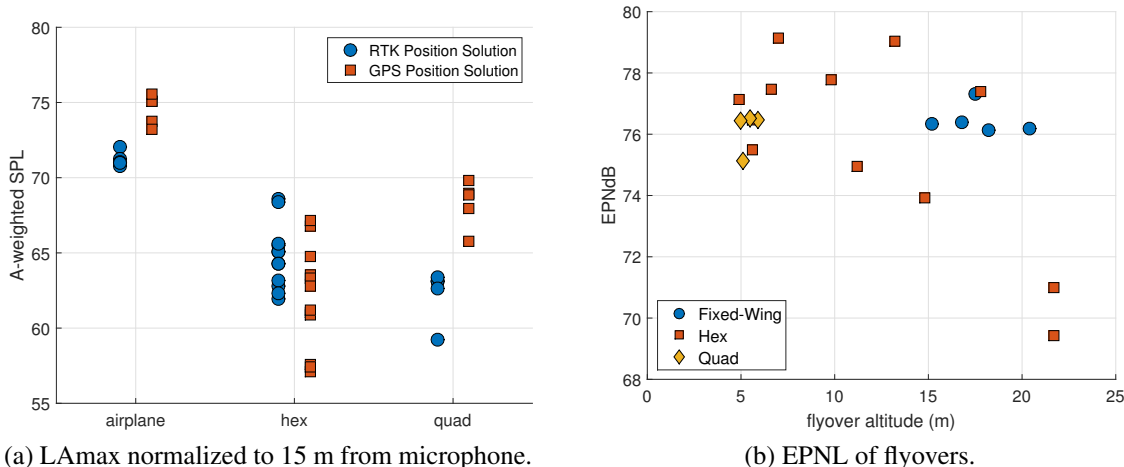


Figure 8: Acoustic metrics of vehicle flyovers

15 m, are shown in Figure 8a for flyovers of three vehicles. The adjustment from the vehicle’s actual height at maximum sound level to 15 m accounted only for spherical spreading. This adjustment required knowledge of the vehicle’s altitude when the maximum sound level occurred. The blue circles show adjusted L_{max} based on measured RTK altitude while the red squares show adjusted L_{max} using GPS altitude. The RTK data is believed to be correct for the flyovers shown in the figure, based on the RTK status bit indicating a good solution and continuity of the RTK position solution during the flyover.

The difference between the RTK and GPS adjusted L_{max} values, particularly for the quadcopter’s relatively low altitude flyovers at about 5 m, illustrates the importance of accurately determining a small vehicle’s position.

The Effective Perceived Noise Level, or EPNL, of small UAV flyovers is shown in Figure 8b. EPNL is a metric defined in aviation regulations that captures aspects of level, frequency, and time duration of vehicle noise, including a penalty for discrete tones.¹² Utilities from NASA’s Aircraft Noise Prediction Program, Version 2 (ANOPP 2) were used to compute EPNL from tone-corrected perceived noise levels of each flyover at 0.5-second intervals.¹³ The *x*-axis in the figure indicates the altitude of the vehicle as it passed over the measurement microphone.

EPNL for the quadcopter and model airplane clustered around 76 EPNdB, although the quadcopter was at about 5 m when it flew over the microphone and the airplane was 15 to 20 m above the microphone. Levels for the hexcopter were much more varied, from a maximum of 79 EPNdB at 7 m to a level of 69.4 EPNdB at 21.7 m.

The Sound Exposure Level (SEL), which is the energy average of a flyover event normalized to a one-second duration¹¹ of the hexcopter flyovers was around 5 dB less than the EPNdB values in Figure 8b. Specifically, the SEL of the two hexcopter flyovers at altitudes 22 m above the microphone were 64.7 and 66 dBA.

4. CONCLUSIONS

Measurements of flyover and hover noise of multicopters and flyover noise of a model airplane were discussed. The spectra for all vehicles are dominated by tones at harmonics of the blade

passage frequency (or frequencies, in the case of the multicopters). Spectrograms showing the variation of acoustic energy with time illustrate the unsteadiness of the noise signatures of these vehicles, particularly for the smallest vehicle, the quadcopter. Although the blade passage frequencies (BPFs) for the multiple rotors on the multicopters are relatively uniform in a hover condition, the BPFs become separated in forward flight as the rotors are driven at different speeds to maintain the vehicle attitude needed for forward motion. Maximum A-weighted sound pressure levels of the vehicles, adjusted to a 15 m altitude flyover, ranged from 63 dBA for the quadcopter to 68 dBA for the hexcopter and 72 dBA for the model airplane. Effective Perceived Noise Levels (EPNL) of flyovers ranged from 76 EPNdB for a 5 m altitude flyover of the quadcopter, to 71 EPNdB for a 22 m altitude flyover of the hexcopter. The extent to which these metrics quantify human annoyance of small vehicles such as these flying in a community is an open question.

REFERENCES

- [1] Hanger 9 edge 540. <http://www.hangar-9.com/Products/Default.aspx?ProdId=HAN1150>. Accessed: 2016-03-14.
- [2] DJI Phantom 2. <http://www.dji.com/product/phantom-2>. Accessed: 2016-03-14.
- [3] 3DR Y6. <https://3dr.com/kb/diy-y6-kit/>. Accessed: 2016-03-14.
- [4] Prioria Hex. <http://www.prioria.com/hex>. Accessed: 2016-03-14.
- [5] 3DR Pixhawk. <https://3dr.com/kb/pixhawk/>. Accessed: 2016-03-14.
- [6] Department of Defense. Global positioning system standard positioning service performance standard. Technical report, DoD Positioning, Navigation, and Timing Executive Committee, September 2008.
- [7] Introducing Piksi. <https://www.swiftnav.com/piksi.html>. Accessed: 2016-03-11.
- [8] B. Magliozzi, D.B. Hanson, and R.K. Amiet. Propeller and propfan noise. In Harvey H. Hubbard, editor, *Aeroacoustics of Flight Vehicles: Theory and Practice: Volume 1: Noise Sources*, number NASA RP-1258, pages 1–64, 1991.
- [9] F.H. Schmitz. Rotor noise. In Harvey H. Hubbard, editor, *Aeroacoustics of Flight Vehicles: Theory and Practice: Volume 1: Noise Sources*, number NASA RP-1258, pages 65–149, 1991.
- [10] Mark Brackley and Charles Pollock. Analysis and reduction of acoustic noise from a brushless dc drive. *IEEE Transactions on Industry Applications*, 36(3):772–777, May/June 2000.
- [11] Clemans A. Powell and James M. Fields. Human response to aircraft noise. In Harvey H. Hubbard, editor, *Aeroacoustics of Flight Vehicles: Theory and Practice: Volume 2: Noise Control*, number NASA RP-1258, pages 1–52, 1991.
- [12] Aircraft noise measurement and evaluation under §36.101. In *Code of Federal Regulations, 14 Pt. 2*, 2005.
- [13] Leonard V. Lopes and Casey L. Burley. Design of the next generation aircraft noise prediction program: ANOPP2. In *17th AIAA/CEAS Aeroacoustics Conference (32nd Aeroacoustics Conference)*, number AIAA 2011-2854, June 2011.